ACS OMEGA

Article

Cite This: ACS Omega 2019, 4, 13418−13425

http://pubs.acs.org/journal/acsodf

Selenite Retention and Cation Coadsorption Effects under Alkaline Conditions Generated by Cementitious Materials: The Case of C−S−H Phases

Tiziana Missana,* Miguel García-Gutiérrez, Manuel Mingarro, and Ursula Alonso

Department of Environment, CIEMAT, Avenida Complutense 40, 28040 Madrid, Spain

Supporting Information

ABSTRACT: Contaminant migration is strongly controlled by sorption reactions; thus, the behavior of anions, which are (almost) not sorbing under alkaline conditions, is an issue of environmental concern. This is especially relevant in the frame of low and intermediate-low radioactive waste repositories, where the pH generated by cement-based materials is hyperalkaline. Selenite (SeO_3^{2-}) sorption on calcium silicate hydrate (C−S−H) phases—the main cement sorbing minerals—has been investigated by batch experiments, ζ-potential measurements, and thermodynamic modeling to elucidate retention mechanisms and possible competitive/synergetic effects of cation coadsorption. Selenite sorption was shown to be nonlinear and slightly increasing with the C−S−H Ca/Si ratio; precipitation of $CaSeO_3$(s) was observed for Se concentration higher than 2×10^{-3} M. Indeed, the presence of Ca is essential to enable selenite retention under alkaline conditions. Progressive additions of Na_2SeO_3 or NaCl salt to the phases produced a change in the C−S−H surface properties, that is, a decrease in the ζ-potential, in apparent agreement with anion adsorption. However, this effect had to be also correlated to Na coadsorption, as Cl showed null retention on the C−S−H phases. At the same time, anion adsorption had a clear effect on the retention of other cations (Ba) in the system. The distribution coefficient of Ba (at trace concentrations) suffered a moderate decrease by the presence of Na^+ and Cl^-, but it was improved by the presence of Na^+ and SeO_3^{2-}, indicating complex competitive/synergetic effects between anions and cations. All of the experimental data were satisfactorily modeled considering a classical double-layer approach.

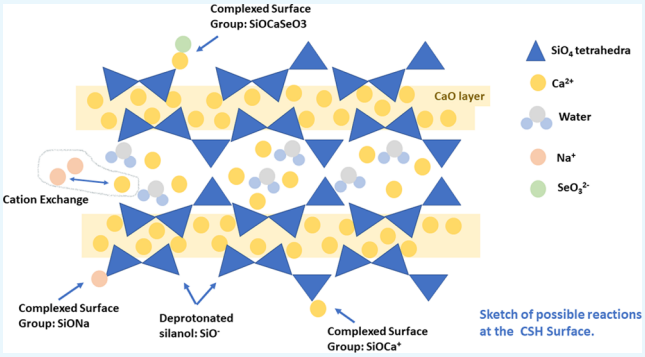

1. INTRODUCTION

The assessment of toxic elements or radioisotopes migration, from disposal sites or contaminated areas, requires an improved knowledge of retention processes and the development of modeling tools for quantitative predictions, trying to account for the complexity of real scenarios.[1]

Anionic species migration is a problem of special concern, as they present low adsorption in natural materials—thus, high mobility—especially under alkaline conditions. Chlorine and iodine are relevant constituents of different types of radioactive waste, and selenium (^{79}Se) is a critical and long-lived ($t_{1/2}$ > 10^5 year) fission product.[2]

In low- and intermediate-low-level radioactive waste repositories, cement-based materials—which generate a hyperalkaline environment—are used for the containment and immobilization of the waste.[3] To assess the long-term safety of these systems, radionuclide (RN) retention mechanisms on cement and its main mineral components must be studied to improve basic knowledge and to be able to develop predictive modeling based on a bottom-up approach.

Calcium silicate hydrate (C−S−H) phases are the major cement hydration products and largely contribute to retention processes because they are amorphous or poorly crystalized materials with a large surface area. They have variable chemical compositions, with their Ca/Si ratio being responsible for the different physical−chemical characteristics.[4]

Previous studies on Cl^- retention in cement-based materials showed that its sorption on hardened cement pastes (HCP) or C−S−H is very weak[5−8] and that its overall retention in HCP depends on the presence of minor phases such as chloroaluminate or hydrotalcite. Baur and Johnson[9] analyzed selenite sorption in various cement minerals, including a C−S−H phase, where they measured distribution coefficients, K_d, of approximately 210 mL g^{-1}. Johnson et al.[10] studied selenite sorption on different cement formulations, reporting K_d values between 250 and 930 mL g^{-1}. They suggested (possibly irreversible) Se surface complexation and observed precipitation at high loadings. On the other hand, Bonhoure et al.[11] analyzed using X-ray absorption spectroscopy the uptake of selenite (at high loadings) onto HCP and cement minerals, inferring nonspecific interactions, and they did not observe selenite precipitation.

Received: June 4, 2019
Accepted: July 23, 2019
Published: August 5, 2019

DOI: 10.1021/acsomega.9b01637
ACS Omega 2019, 4, 13418−13425

Table 1. Chemical Analyses of the Supernatant of the C−S−H Phases[a]

sample	pH	conductivity (μS cm^{-1})	Ca (mg L^{-1})	Si (mg L^{-1})
C−S−H (0.8)	10.33 ± 0.10	196 ± 7	44 ± 4	73 ±1 1
C−S−H (1.0)	11.51 ± 0.10	1080 ± 100	96 ± 8	3.5 ± 0.5
C−S−H (1.2)	12.06 ± 0.20	2350 ± 100	216 ± 10	1.7 ± 0.3
C−S−H (1.6)	12.34 ± 0.10	6150 ± 100	572 ± 25	0.16 ± 0.05

[a]The mean values are obtained considering different preparations.

Thus, despite the number of papers qualitatively describing sorption processes of (oxy)anions on cementitious materials, the mechanisms of their interactions are not yet very well established[5] and, to the best of our knowledge, literature on detailed modeling of selenite retention in C−S−H phases, including possible additional interaction effects with other adsorbing ions, especially cations, is not available.

C−S−H phases may show different affinities for anions or cations, as the sign of their surface charge varies with the Ca/Si ratio.[12−15] Anion and cations can be simultaneously adsorbed on the phases to a different extent, but C−S−H with low Ca/Si ratios, presenting negative surface charge, should retain preferentially cations, whereas gels with higher Ca/Si ratios are expected to better retain anions.

Because of the complexity of C−S−H surface, the diversity of possible sorption mechanisms, and the competitive effects (among different anions and/or anions and cations), sorption processes on C−S−H are not straightforward to understand. Their mechanistic description is challenging but necessary for the development of predictive models.

The aim of this study is to analyze the adsorption of SeO_3^{2-} (and Cl^-) in C−S−H phases with different Ca/Si ratios, analyzing also cation coadsorption and possible competing effects. Different sets of batch sorption experiments and electrophoretic measurements were carried out to discern possible underlying interaction mechanisms and to describe them by surface complexation modeling.

2. EXPERIMENTAL SECTION

2.1. C−S−H Gels Preparation and Characterization. C−S−H phases with different CaO/SiO_2 (Ca/Si) molar ratios were prepared, with the Ca/Si targets being 0.8, 1, 1.2, and 1.6 (C−S−H (0.8); C−S−H (1); C−S−H (1.2); and C−S−H (1.6)). Their synthesis and all sorption experiments were carried out in a glovebox, under N_2 atmosphere (O_2 < 1 ppm) to avoid surface carbonation and to maintain the equilibrium pH. More details on preparation can be found in a previously published work.[15]

The final pH and conductivity of the supernatant of C−S−H suspensions, as well as Ca and Si concentrations, are specific for each Ca/Si ratio and are summarized in Table 1.

The different compositions of the C−S−H phases and their pH values are related to different stages of cement degradation.

The mean N_2-Brunauer−Emmett−Teller surface area measured for C−S−H (0.8), C−S−H (1), and C−S−H (1.2) was 144 ± 40 m^2 g^{-1}; the mean value measured for C−S−H (1.6) was approximately halved (73 m^2 g^{-1}) due to portlandite precipitation, as previously discussed.[15]

2.2. ζ-Potential and Particle Size Measurements. The ζ-potential of the C−S−H phases (1 g L^{-1}) was measured by laser Doppler electrophoresis using a Malvern Zetamaster apparatus (5 mW He−Ne laser, λ = 633 nm at a scattering angle of 90°). The ζ-potential was calculated from the measured electrophoretic mobility using the Smoluchowski equation.[16]

To analyze the behavior of the ζ-potential, upon chloride and selenite addition (from 1 × 10^{-3} to 4 × 10^{-2} M), NaCl and Na_2SeO_3 salts of high purity were used; the measurements were performed 3 days after salts addition, and during this contact period, the suspensions were maintained by stirring in the anoxic glovebox.

C−S−H particle size was measured with a Malvern ZetaSizer Nano ZS (5 mW He−Ne laser, λ = 633 nm at a scattering angle of 173°). In all of the phases, the particles have sizes smaller than 100 nm[15] but form aggregates with average size larger than 1 μm because of the aqueous Ca content.

2.3. Batch Sorption Tests. Sorption data were obtained using the radioisotopes ^{75}Se and ^{36}Cl. Carrier-free selenite stock solution (as H_2SeO_3) was supplied by Isotope Products. ^{75}Se is a gamma-emitter (136 and 256 keV) with a half-life of about 120 days; its activity was measured by γ-counting with a NaI detector (Packard Autogamma COBRA II).

^{36}Cl was supplied in NaCl form, dissolved in pure water (Isotope Products). It is a β-emitter with half-life of 3.01 × 10^5 years. Its activity was measured by liquid scintillation counting with a PerkinElmer Tricarb 4910-TR apparatus.

Sorption experiments with the different C−S−H phases (10 g L^{-1}) were carried out in an anoxic glovebox under N_2 atmosphere and at room temperature with the samples in triplicate. Sorption kinetics was initially investigated to determine the time required for the attainment of the sorption equilibrium, and samples were maintained under continuous stirring during the selected contact time (from 1 to 90 days) with a rotative mixer (Rotator SB2, Stuart). In kinetic tests, the RN concentrations were: [Se] = 1.3 × 10^{-6} M and [Cl] = 8.0 × 10^{-7} M.

Sorption isotherms of ^{75}Se were carried out with the four C−S−H phases, with [Se] ranging from 5 × 10^{-7} to 1 × 10^{-2} M approximately. Higher Se concentrations were achieved by adding stable Na_2SeO_3. Sorption isotherms under similar experimental conditions were also carried out with ^{36}Cl. The contact time for sorption isotherms was fixed to 10 days.

The solid and liquid phases were separated by centrifuging (25 000g, 30 min) with a JOUAN MR23i centrifuge. After the solid separation, three aliquots of the supernatant were extracted from each tube for the analysis of the final Se or Cl activity. The rest of the solution was used to check the final pH.

Distribution coefficients, K_d (mL g^{-1}), were calculated as

$$K_d = \frac{C_{in} - C_{fin}}{C_{fin}} \cdot \frac{V}{m} \quad (1)$$

where C_{in} and C_{fin} are the initial and final concentrations of tracer in the liquid phase (counts mL^{-1}), respectively, m is the mass of the gel (g), and V is the volume of the liquid (mL).

DOI: 10.1021/acsomega.9b01637
ACS Omega 2019, 4, 13418−13425

It can be anticipated that K_d's measured for ^{36}Cl in all of the C−S−H gels were null within the experimental error (K_d < 2 mL g^{-1}), in agreement with previous studies.[5,7,8]

Competition effects on cation adsorption due to the presence of Cl^- and SeO_3^{2-} (from approximately 1 × 10^{-3} to 5 × 10^{-2} M), in the form of NaCl and Na_2SeO_3, were carried out by measuring K_d values of ^{133}Ba ([Ba] = 3.4 × 10^{-10} M) as a function of salts concentration. Barium was in the form of $BaCl_2$ in HCl 0.1 M with a carrier of stable Ba (10 μg mL^{-1} solution); ^{133}Ba has a half-life of 10.51 years, and its activity in solution was measured by γ-counting with a NaI detector (Packard Autogamma COBRA II).

Barium was selected as reference trace cation in anion−cation coadsorption tests as its sorption behavior was previously analyzed and modeled in detail.[15]

2.4. Sorption Modeling. A classical diffuse double-layer approach was used for describing surface complexation reactions.[17,18] The relationship between the diffuse potential, ψ, and charge density, σ, is given (for a symmetric electrolyte) by

$$\sigma = -0.1174 \cdot \sqrt{I} \cdot \sinh\left(\frac{ze\Psi}{2kT}\right) \quad (2)$$

In this expression, σ is given in C m^{-2}, Ψ in V, k is the Boltzmann constant, T is the absolute temperature, e is the electron charge, z is the electrolyte valence, and/is the ionic strength of the solution in mol L^{-1}. To support the modeling, the calculated diffuse layer potential was compared to the experimentally determined ζ-potential.[16,19]

Model calculations were performed using the geochemical CHESS v. 2.4 code,[20] and the geochemical database was the standard EQ3/6; the constants for selenite were revised according to Séby et al.[21]

3. RESULTS AND DISCUSSION

3.1. Batch Sorption Studies. As adsorption of ^{36}Cl was negligible (K_d < 2 mL g^{-1}) in all of the C−S−H phases, it can be considered as an indifferent ion.

The adsorption kinetics of ^{75}Se in the C−S−H phases with Ca/Si ratios of 0.8, 1.2, and 1.6 was analyzed first (Figure S1, Supporting Information). Sorption equilibrium was reached in a few hours in the C−S−H phases with Ca/Si ratios of 1.2 and 1.6 and in a few days in C−S−H (0.8). No signals of slower uptake mechanisms or desorption processes were observed within the analyzed time frame of 3 months. According to these data, the selected contact time for sorption isotherms was 10 days.

Second, sorption isotherms were carried out and the final pH values after the tests were 10.30 ± 0.02, 11.72 ± 0.02, 12.00 ± 0.05, and 12.38 ± 0.03 for the C−S−H phases 0.8, 1, 1.2, and 1.6, respectively.

The results of selenite sorption isotherms are shown in Figure 1, where data are expressed as the logarithm of adsorbed Se per unit mass in mol g^{-1}, $Log[Se]_{ads}$, vs the logarithm of Se concentration in the liquid phase at the equilibrium in mol L^{-1}, $Log[Se_{eq}]$.

Selenite sorption depends on Se concentration, being nonlinear, as shown by K_d values variation. The highest K_d (110 g mL^{-1}) is measured at the lowest Se concentration and the highest Ca/Si ratio; the lowest K_d (11 g mL^{-1}) is measured at a Se concentration of approximately 10^{-3} M and at the lowest Ca/Si ratio.

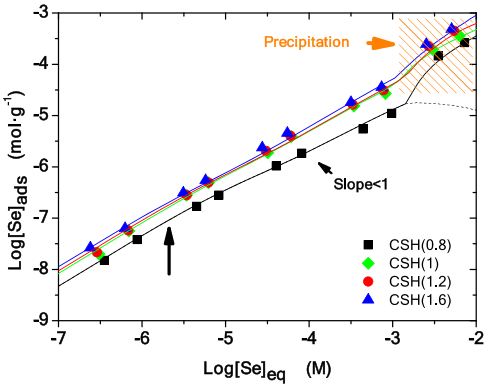

Figure 1. Sorption isotherms for selenite in the C−S−H phases (10 g L^{-1}): (■) C−S−H (0.8); (green tilted square solid) C−S−H (1); (red circle solid) C−-S−H (1.2); and (sky blue triangle up solid) C−S−H (1.6). The continuous lines correspond to model calculations (Section 3.4, Tables S1, and Table 2). The dashed box corresponds to the region in which $CaSeO_3$ precipitation is observed. The dashed line represents the theoretical sorption behavior if precipitation is not included in the modeling.

The C−S−H phases with higher Ca content are better sorbent solids for selenite even the main difference is observed for C−S−H (0.8), which clearly adsorbs less than the others. K_d values obtained for selenite range between 50 and 100 mL g^{-1} approximately within the range reported in the review by Ochs et al.[5]

Additionally, Figure 1 shows that sorption isotherms present a first slight change in slope at Se equilibrium concentration of around 5 × 10^{-6} M (black arrow), indicating that sorption sites of "low" density might be saturating. Thus, the shape of the isotherm suggests the existence of—at least—two sorption sites for selenite sorption. As selenite concentration increases further, K_d values progressively decrease (the slope of the lines in the graph is <1). Finally, at a concentration of approximately 2−5 × 10^{-3} M, a sharp increase in the slope is detected. This last behavior must be related to the precipitation of a solid phase, most probably $CaSeO_3$.

X-ray diffraction measurements of the phases upon selenite addition at high concentrations were performed. Despite the difficulties of recognizing (trace) phases within essentially amorphous solids, such as C−S−H gels, the main lines of $CaSeO_3 \cdot H_2O$ could be identified.

3.2. ζ-Potential Measurements. ζ-Potential measurements were carried out before and upon the addition of increasing concentration of salts (NaCl and Na_2SeO_3). The initial ζ-potentials (in mV) of the C−S−H were −11.7 ± 3.0, −3.0 ± 0.5, 4.5 ± 1.0, and 11.7 ± 3.0 for the Ca/Si ratios of 0.8, 1, 1.2, and 1.6, respectively.

The charge of C−S−H depends on the Ca/Si ratio:[12,15] at the lower Ca/Si ratios (corresponding to lower aqueous Ca), the charge is negative; as the solute Ca and Ca/Si increase, the charge evolves toward more positive values. This can be explained considering that Ca^{2+} is the ion determining the potential (IDP) of the C−S−H phases.[12,15]

The variations of the ζ-potential observed upon the addition of different salts NaCl or Na_2SeO_3 are described in Figure 2. Selenite precipitation may somewhat bias the results of electrokinetic measurements for Se concentrations higher than 10^{-3} M, even if the contact time of these experiments was shorter (3 days instead of 10 days adopted for the sorption

DOI: 10.1021/acsomega.9b01637
ACS Omega 2019, 4, 13418−13425

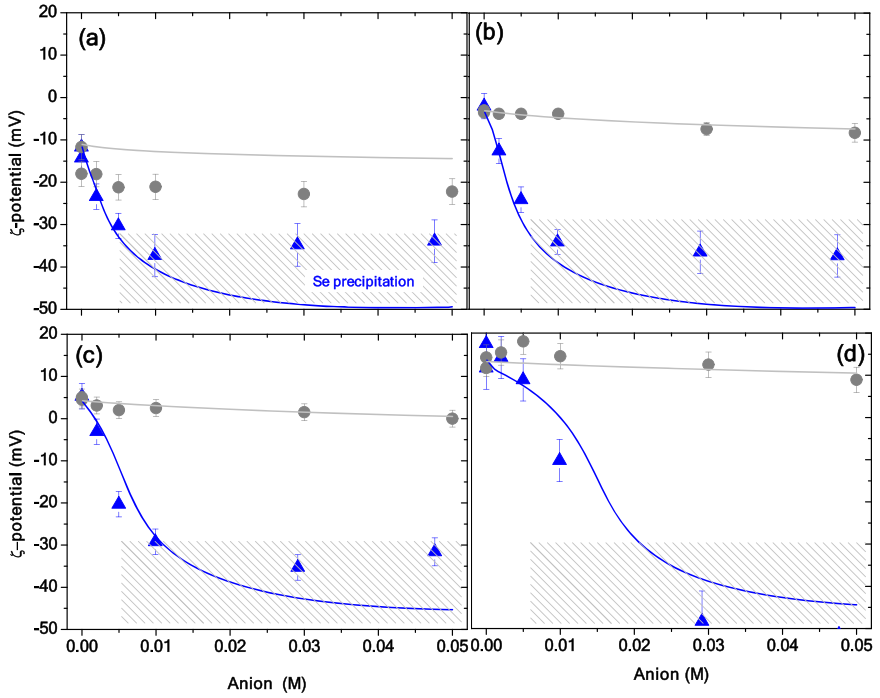

Figure 2. ζ-Potential variation upon the addition of anions in the form of (gray circle solid) NaCl and (sky blue triangle up solid) Na_2SeO_3 to the different C−S−H phases (1 g L^{-1}): (a) C−S−H (0.8), (b) C−S−H (1), (c) C−S−H (1.2), and (d) C−S−H (1.6). The continuous lines correspond to model calculations (Section 3.4, Table S1, and Table 2).

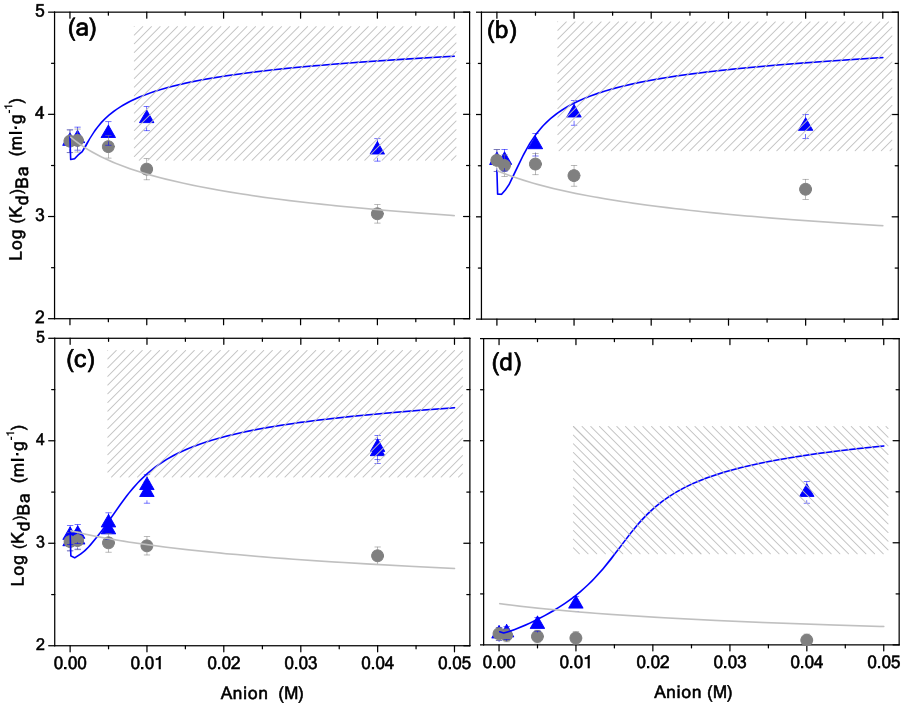

Figure 3. Variation of K_d for Ba ([Ba] = 3.4 × 10^{-10} M) upon the addition of anions in the form of (gray circle solid) NaCl and (sky blue triangle up solid) Na_2SeO_3 to the different C−S−H phases (10 g L^{-1}): (a) C−S−H (0.8), (b) C−S−H (1), (c) C−S−H (1.2), and (d) C−S−H (1.6). The continuous lines correspond to model calculations (Section 3.4, Tables S1, and 2).

isotherms). The zone of possible selenite precipitation is marked with a gray rectangle.

In all of the cases, upon salts addition, the ζ-potential of the C−S−H phases tends to decrease toward more negative values, and in principle, this would agree with the (specific) adsorption of anionic species.[22,23] Nevertheless, as Cl^- has been shown to be an "indifferent" ion, the overall effect on the surface charge must be caused both by the adsorption of the anions and by the counter-cation Na,[24] which will be accounted for in the overall analysis of data.

3.3. Effect of the Presence of Anions on Ba Adsorption in the C−S−H Phases. Sorption experiments

DOI: 10.1021/acsomega.9b01637
ACS Omega 2019, 4, 13418−13425

with Ba, at a trace concentration, in the presence of increasing concentrations of Na_2SeO_3 and NaCl were carried out to understand the possible role of anions on cation adsorption in the different C−S−H phases. Figure 3 shows the variation of K_d values for Ba, at increasing salt concentrations. Again, the zone of possible selenite precipitation is marked with a gray rectangle.

The presence of the two salts causes different effects on Ba adsorption: when NaCl is added, the distribution coefficients of Ba tend to decrease slightly, whereas upon Na_2SeO_3 addition, Ba sorption increases.

Considering that Na is a mildly sorbing element in the C−S−H phases[24] and Cl is not sorbing (Section 3.1), the small decrease in Ba adsorption upon the NaCl addition (Figure 3) could be interpreted by the competitive effect of the two cations Na and Ba. However, a double quantity of Na for a mol of anion is present upon Na_2SeO_3 addition; therefore, a stronger competitive effect might be foreseen. But the presence of selenite favors Ba retention in all of the C−S−H phases.

This different behavior must depend on the relative strength of the complexes formed with the C−S−H sorption sites and on their relative occupancy.

Indeed, the overall charge clearly decreases when Na_2SeO_3 is added to the C−S−H phases (Figure 2), and this must favor cation retention. A similar effect was observed in refs25, 26, where it was reported that the selenite coadsorption altered Co retention on γ-alumina, depending on the selenite surface coverage: at low Se surface coverage, no changes in Co sorption were detectable, but at higher Se loadings, Co sorption increased. Electrostatic enhancement mechanisms, ternary complexes formation, or surface coprecipitation were considered as possible causes of these results.

Yet, the overall behavior caused by Ba, Na, and selenite coadsorption is very difficult to predict without detailed experiments and theoretical modeling efforts, which may help discover possible mechanisms involved.

3.4. Modeling. To be suitable to predict RN behavior in more complex systems, an adequate sorption model should catch at least the main peculiarities observed in the different types of experimental data. In the present study, it must fit: (a) the sorption dependence on Se concentration and on C−S−H Ca/Si ratio (Figure 1); (b) the variation of the ζ-potential (Figure 2); and (c) variation of distribution coefficient for Ba (Figure 3), as Na_2SeO_3 or NaCl concentration increases in the system.

The surface properties of the C−S−H phases needed for sorption modeling were already defined in ref15 and are summarized in Table S1 (Supporting Information); they were fixed in the model. The adsorption behavior of Na on these C−S−H phases was analyzed in a previous paper:[24] the parameters used to account for Na coadsorption are included in Table S1 and fixed as well.

More details on the determination of these parameters can be found in refs15, 24. Briefly, up to three different sites for cation adsorption may exist on the C−S−H surface: two types of silanol sites (SiOH) with different selectivity for cations (strong, S, and weak, W) and ion-exchange sites, E, initially occupied by Ca (X_2Ca). Ca is postulated as an ion determining the potential (IDP). The densities of W and S silanol sites are 13 and 3.5×10^{-3} μmol m^{-2}, respectively, and the density of E sites is 2 μmol m^{-2}.

For anion adsorption, cation-exchange sites (X_2Ca) are not "active"; therefore, only the surface complexation sites (SiOH, W, and S) were considered. Under alkaline conditions, the silanol-like sites, SiOH, at the C−S−H surface are deprotonated according to the following reaction

$$SiOH \leftrightarrow SiO^- + H^+ \quad (3)$$

Ca is the ion determining the potential (IDP) of the C−S−H phases; therefore, of special importance is the reaction between the deprotonated silanols-like groups and Ca

$$SiO^- + Ca^{2+} \Leftrightarrow SiOCa^+ \quad (4)$$

Focusing on anion retention, several studies are available describing (oxy)anion complexation on oxides, especially for selenium (ref27 and references therein). Selenite species ($HSeO_3^-$ and SeO_3^{2-}) are often reported to form inner-sphere complexes with the mineral surface sites (S−OH) according to reactions of this type[28]

$$S - OH_2^+ + SeO_3^{2-} \Leftrightarrow S - SeO_3^- + H_2O \quad (5a)$$

$$S - OH_2^+ + HSeO_3^- \Leftrightarrow S - HSeO_3 + H_2O \quad (5b)$$

Thus, according to the anionic nature of its species, selenium sorption is generally modeled considering complexation with the protonated surface sites, $S-OH_2^+$ (eqs 5a and 5b).

In the case of C−S−H phases, pH conditions are strongly alkaline, and surface functional groups are mainly deprotonated (eq 3); therefore, the direct complexation of anions with the silanol-like sites of C−S−H is unlikely. Furthermore, the $HSeO_3^-$ species (eq 5a) can be neglected at very high pH, where the main aqueous species is SeO_3^{2-}.

Preliminary modeling included trials considering eqs 5a and 5b but, in the end, best and credible results were obtained postulating that selenite adsorption on the C−S−H phases depends on the formation of complexes between SeO_3^{2-} and silanol-like surface sites, where Ca^{2+} is already adsorbed (eq 4).[29,30]

The chemical reaction used to describe anion complexation in the C−S−H phases, extensive to any (oxy)anion, An^{n-}, is the following

$$SiOCa^+ + An^{n-} \leftrightarrow SiOCaAn^{(n-1)-} \quad (6)$$

The main hypothesis for the selenite sorption model is that the anion complexation with the C−S−H surface obeys the reaction described in eq 6, evidencing the great importance of the presence of Ca on selenite retention under alkaline conditions.

Second, the shape of the selenite sorption isotherms indicates that sorption is not linear and that a contribution of "strong" sites to the overall sorption must exist.

The sorption model was tested on selenite sorption data adjusting the fit parameters, and considering, in parallel, its validity on electrokinetic (Figure 2) and Ba sorption (Figure 3) data.

Figure 4 shows the summary of the simulations obtained for the selenite sorption isotherms (Figure 4a) and for the behavior of the electrokinetic potential and the distribution coefficient of Ba ($[Ba] = 3.4 \times 10^{-10}$ M) as a function of Na_2SeO_3 addition (Figure 4b,c, respectively). In these two figures, used for modeling purposes, the range of Se concentration was limited to $[Se] < 1 \times 10^{-2}$ M because for higher concentrations, the existence of precipitation was detected. In any case, the simulations for the entire range of experimental concentrations have also been included in Figure 2 (ζ-potential) and Figure 3 (Ba adsorption).

DOI: 10.1021/acsomega.9b01637
ACS Omega 2019, 4, 13418−13425

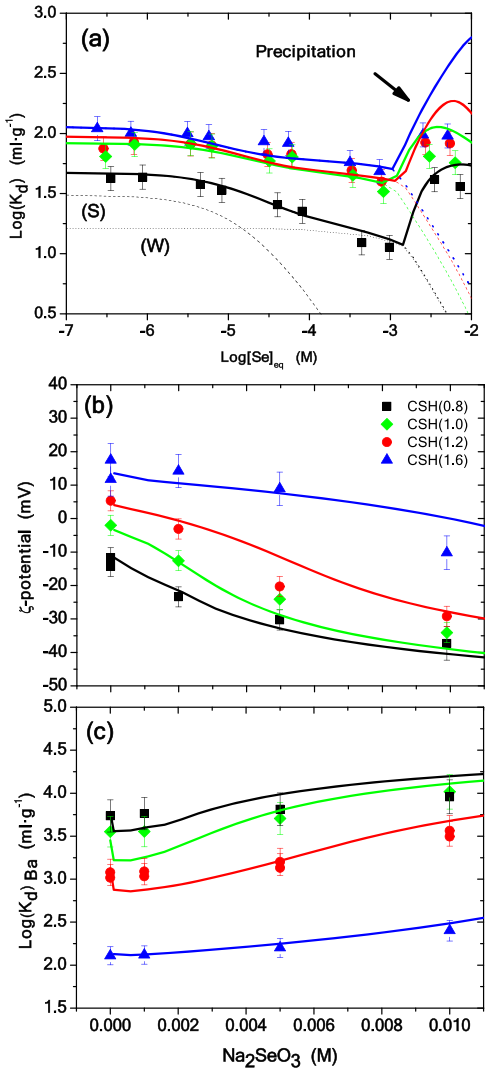

Figure 4. Modeling of the entire set of selenite data. (a) Sorption isotherms, (b) ζ-potential, and (c) barium K_d variation upon the addition of Na_2SeO_3. (■) C−S−H (0.8), (green tilted square solid) C−S−H (1), (red circle solid) C−S−H (1.2), and (sky blue triangle up solid) C−S−H (1.6). The continuous lines correspond to model calculations (parameters in Tables S1 and Table 2). The dotted lines in (a) correspond to the model of sorption excluding $CaSeO_3$ precipitation. In the modeling of C−S−H (0.8), the contribution of weak (W) and strong (S) sites is evidenced.

The sorption isotherms in Figure 4a are expressed as the logarithm of K_d (mL g^{-1}), (Log(K_d)) vs logarithm of solute selenium concentration at equilibrium, in mol L^{-1} (log[Se_{eq}]), because with this representation, modeling results as well as the observed nonlinear sorption behavior are much clearer.

Table 2 summarizes the reaction and parameters used for simulating the interactions of selenite with the C−S−H phases, and the model calculations are superimposed to experimental data in Figure 4 as continuous lines. The contribution of weak (W) and strong (S) sites to sorption, for C−S−H (0.8), is evidenced in the graph.

As can be seen in Figure 4a, the model reproduces quite well the selenite adsorption data in all of the C−S−H phases. The mean values for the complexation constants (eq 6) for all of the C−S−H phases are 1.55 ± 0.17 and −1.78 ± 0.27 for strong and weak sites, respectively (Table 2). Even if the standard deviation for the parameters determined in the different C−S−H phases is not higher than 15%, a clear shift is observed in the complexation constants with the Ca/Si ratio: the constants tend to increase as the Ca/Si ratio increases, which might be an indication that the surface structure of C−S−H depends somewhat on the Ca/Si ratio, which deserves more detailed studies.

The sharp increase of K_d values observed at selenite concentrations higher than 1×10^{-3} M can be fit reasonably well considering the formation of $CaSeO_3$ (s) with a constant of 6.3 ± 0.2. This value is lower than the value of 7.6 recommended by Séby et al.,[21] but it is in the range of values reported in the literature and agrees quite well with the one recently proposed in the database review of Thoenen et al. of 6.40 ± 0.25.[31]

Without the precipitation of this solid, selenite sorption would continuously decrease, as indicated by the dotted curves in Figure 4a.

The model is also able to well predict the variation of the surface potential upon Na_2SeO_3 addition for all of the C−S−H phases (Figure 4b) and the experimentally observed increase of Ba retention in the presence of the selenite Na salt (Figure 4c).

The interactions of selenite with the C−S−H surface caused a decrease of their surface charge, toward more negative values, affecting the coadsorption of other species. Ba adsorption suffered a moderate decrease by the presence of Na^+ and Cl^- (the latter not sorbing on the C−S−H phases) but was improved by the presence of Na^+ and SeO_3^{2-}. Nevertheless, in Figure 4c, it can be pointed out that for the phases with Ca/Si of 0.8, 1, and 1.2, at very low salt concentration, an initial (slight) decrease for Ba sorption is predicted by the model. Thus, both competitive and synergetic effects can be observed in this system.

Table 2. Reactions and Parameters Used to Define Selenite Retention in the C−S−H Phases

description	surface species (CHESS code)	log K	mean log K	refs
sorption of SeO_3^{2-} in S	$Si_sOCaSeO_3^-$ = 1 Si_sOH, −1 H^+, 1 Ca^{2+}, 1 SeO_3^{2-}	C−S−H (0.8) 1.45	1.55 ± 0.17	this work
		C−S−H (1.0) 1.45		
		C−S−H (1.2) 1.50		
		C−S−H (1.6) 1.80		
sorption of SeO_3^{2-} in W	$Si_wOCaSeO_3^-$ = 1 Si_wOH, −1 H^+, 1 Ca^{2+}, 1 SeO_3^{2-}	C−S−H (0.8) −2.10	−1.78 ± 0.27	this work
		C−S−H (1.0) −1.75		
		C−S−H (1.2) −1.80		
		C−S−H (1.6) −1.45		
$CaSeO_3$ precipitation	$CaSeO_3$(s) = 1 Ca^{2+}, 1 SeO_3^{2-}	6.3 ± 0.2		this work

DOI: 10.1021/acsomega.9b01637
ACS Omega 2019, 4, 13418−13425

4. CONCLUSIONS

Selenite (SeO_3^{2-}) sorption on C−S−H phases of different Ca/Si ratios (0.8, 1, 1.2, and 1.6) has been analyzed by different techniques. Sorption slightly depended on the Ca/Si ratio, with K_d values ranging between 10 and 100 mL g^{-1} approximately.

The interaction of selenite with the C−S−H phases causes a non-negligible decrease of their surface charge, which affects the coadsorption of other species present in solution. Both competitive and synergetic effects were observed in the system. These effects, which are expected to occur in complex materials such as cements and to be relevant in the overall radionuclide retention, can be predicted only by a detailed analysis of experimental data and appropriate modeling.

The integration of different experiments is fundamental to explain RN retention on complex systems such as cements and is necessary for validation of sorption models. In this work, three different sets of data were used to understand the overall behavior of selenite sorption on the C−S−H phases and competitive/synergetic effects with other cations in solution. The final modeling adequately fits all sets of data.

This study revealed that the role of Ca on selenite sorption on C−S−H is especially important, as it allows selenite retention under hyperalkaline conditions where, otherwise, it would be hindered. At low-medium loadings, selenite adsorption is driven by complexed Ca^{2+}; at high loadings, selenite coprecipitation with Ca represents an additional important retention process, controlling the overall mobility of the anion.

■ ASSOCIATED CONTENT

Supporting Information

The Supporting Information is available free of charge on the ACS Publications website at DOI: 10.1021/acsomega.9b01637.

Sorption kinetics of Se(IV) on different C−S−H phases; reactions and parameters used in the modeling to define the C−S−H surface and Na coadsorption (PDF)

■ AUTHOR INFORMATION

Corresponding Author

*E-mail: tiziana.missana@ciemat.es.

ORCID

Tiziana Missana: 0000-0003-3052-5185

Notes

The authors declare no competing financial interest.

■ ACKNOWLEDGMENTS

This work was partially supported by the Spanish Ministry of Economy, Industry and Competitiveness within the grant CTM2014-60482-P (MIRAME project) and the European Commission EURAD Programme (Grant Agreement no. 847593). The Division of Chemistry of CIEMAT is acknowledged for its support in chemical analyses.

■ REFERENCES

(1) Payne, T.; Brendler, V.; Ochs, M.; Baeyens, B.; Browne, P. L.; Davis, J. A.; Ekbergg, C. E.; Kulik, D. A.; Lutzenkirchen, J.; Missana, T.; Tachi, Y.; Van Loon, L.; Altmann, S. Guidelines for thermodynamic sorption modelling in the context of radioactive waste disposal. *Environ. Modell. Software* **2013**, *42*, 143−156.

(2) Séby, F.; Potin-Gautier, M.; Giffaut, E.; Donard, O. Assessing the speciation and the biogeochemical processes affecting the mobility of selenium from a geological repository of radioactive wastes to the biosphere. *Analusis* **1998**, *26*, 193−198.

(3) Chen, Q. Y.; Tyrer, M.; Hills, C. D.; Yang, X. M.; Carey, P. Immobilisation of heavy metals in cement-based solidification/stabilisation: a review. *Waste Manage.* **2009**, *29*, 390−403.

(4) Chen, J. J.; Thomas, J. J.; Taylor, H. F. W.; Jennings, H. M. Solubility and structure of calcium silicate hydrate. *Cem. Concr. Res.* **2004**, *34*, 1499−1519.

(5) Ochs, M.; Mallants, D.; Wang, L. Radionuclide and Metal Sorption on Cement and Concrete. In *Topics in Safety, Risk, Reliability and Quality*; Springer, 2016; Vol. *29*, pp 301, ISBN 978-3-319-23650-6.

(6) Pointeau, I.; Coreau, N.; Reiller, P. E. Uptake of anionic radionuclides onto degraded cement pastes and competing effects of organic ligands. *Radiochim. Acta* **2008**, *96*, 367−374.

(7) Aggarwal, S.; Angus, M. J.; Ketchen, J. *Sorption of Radionuclides onto Specific Mineral Phases Present in Repository Cements*; Technical Report NSS/R312, AEA-D&R-0395, 2000.

(8) Kalinichev, A. G.; Kirpatrick, R. J. Molecular dynamic modelling of chloride binding to the surfaces of calcium hydroxide, hydrated calcium aluminate and calcium silicate phases. *Chem. Mater.* **2002**, *14*, 3539−3549.

(9) Baur, I.; Johnson, C. A. Sorption of selenite and selenate to cement minerals. *Environ. Sci. Technol.* **2003**, *37*, 3442−3447.

(10) Johnson, E. A.; Rudin, M. J.; Steinberg, S. M.; Johnson, W. H. The sorption of selenite on various cement formulations. *Waste Manage.* **2000**, *20*, 509−516.

(11) Bonhoure, I.; Baur, I.; Wieland, E.; Johnson, C. A.; Sheidegger, A. M. Uptake of Se(IV/VI) oxyanions by hardened cement pastes and cement minerals: an X-ray absorption spectroscopy study. *Cem. Concr. Res.* **2006**, *36*, 91−98.

(12) Viallis-Terrisse, H.; Nonat, A.; Petit, J. C. Zeta-Potential Study of Calcium Silicate Hydrates Interacting with Alkaline Cations. *J. Colloid Interface Sci.* **2001**, *244*, 58−65.

(13) Pointeau, I.; Reiller, P.; Macé, N.; Landesman, C.; Coreau, N. Measurement and modelling of the surface potential evolution of hydrated cement pastes as a function of degradation. *J. Colloid Interface Sci.* **2006**, *300*, 33−44.

(14) Henocq, P. A sorption model for alkalis in cement-based materials − correlations with solubility and electrokinetic properties. *Phys. Chem. Earth* **2017**, *99*, 184−193.

(15) Missana, T.; García-Gutiérrez, M.; Mingarro, M.; Alonso, U. Analysis of barium retention mechanisms on calcium silicate hydrate phases. *Cem. Concr. Res.* **2017**, *93*, 8−16.

(16) Hunter, R. J. *Zeta Potential in Colloid Science*, 1st ed.; Academic Press, 1981; pp 398.

(17) Huang, C. P.; Stumm, W. Specific adsorption of cations hydrous Al_2O_3. *J. Colloid Interface Sci.* **1973**, *43*, 409−420.

(18) Dzombak, D. A.; Morel, F. M. *Surface Complexation Modelling: Hydrous Ferric Oxide*; John Wiley & Sons, 1990.

(19) Delgado, A. V.; González-Caballero, F.; Hunter, R. J.; Koopal, L. K.; Lyklema, J. Mesurement and interpretation of electrokinetic phenomena. *J. Colloid Interface Sci.* **2007**, *309*, 194−224.

(20) Van der Lee, J.; de Windt, L. *CHESS Tutorial and Cookbook*; Technical Report LHM/RD/99/05, 1999.

(21) Séby, F.; Potin-Gautier, M.; Giffaut, E.; Borge, G.; Donard, O. F. X. A critical review of thermodynamic data for selenium species at 25 °C. *Chem. Geol.* **2001**, *171*, 173−194.

(22) Hansmann, D. D.; Anderson, M. A. Using electrophoresis in modelling sulphate, selenite and phosphate adsorption onto goethite. *Environ. Sci. Technol.* **1985**, *19*, 544−551.

(23) Su, C.; Suarez, D. L. Selenate and selenite sorption on iron oxides: an infrared and electrophoretic study. *Soil Sci. Soc. Am. J.* **2000**, *64*, 101−111.

(24) Missana, T.; García-Gutiérrez, M.; Mingarro, M.; Alonso, U. Comparison between cesium and sodium retention on calcium silicate hydrate phases. *Appl. Geochem.* **2018**, *98*, 36−44.

DOI: 10.1021/acsomega.9b01637
ACS Omega 2019, 4, 13418−13425

(25) Boyle-Wight, E. J.; Katz, L. E.; Hayes, K. F. Macroscopic studies of the effects of selenate and selenite on cobalt adsorption to gamma-alumina. *Environ. Sci. Technol.* **2002**, *36*, 1212−1218.
(26) Boyle-Wight, E. J.; Katz, L. E.; Hayes, K. F. Spectroscopic studies of the effects of selenate and selenite on cobalt adsorption to gamma-alumina. *Environ. Sci. Technol.* **2002**, *36*, 1219−1225.
(27) Mayordomo, N.; Foerstendorf, H.; Lutzenkirchen, J.; Heim, K.; Weiss, S.; Alonso, U.; Missana, T.; Schmeide, K.; Jordan, M. Selenium(IV) Sorption Onto γ-Al2O3: A Consistent Description of the Surface Speciation by Spectroscopy and Thermodynamic Modelling. *Environ. Sci. Technol.* **2018**, *52*, 581−588.
(28) Balistrieri, L. S.; Chao, T. T. Selenium adsorption by goethite. *Soil Sci. Soc. Am. J.* **1987**, *51*, 1145−1151.
(29) Noshita, K.; Nishi, T.; Matsuda, M.; Izumida, T. Sorption mechanisms of carbon-14 by hardened cement paste. *Mater. Res. Soc. Symp. Proc.* **1995**, *412*, No. 435.
(30) Pointeau, I.; Hainos, D.; Coreau, N.; Reiller, P. Effects of organics on selenite uptake by cementitious materials. *Waste Manage.* **2006**, *26*, 733−740.
(31) Thoenen, T.; Hummel, W.; Berner, U.; Curti, E. *The PSI/Nagra Chemical Thermodynamic Database 12/07*; Technical Report Nr. 14-04, 2014.

DOI: 10.1021/acsomega.9b01637
ACS Omega 2019, 4, 13418−13425